



A fluorometric turn-on aptasensor for mucin 1 based on signal amplification via a hybridization chain reaction and the interaction between a luminescent ruthenium(II) complex and CdZnTeS quantum dots

Zheng Li¹ · Guobin Mao¹ · Mingyuan Du¹ · Songbai Tian¹ · Longqing Niu¹ · Xinghu Ji¹ · Zhike He¹

Received: 28 November 2018 / Accepted: 27 February 2019 / Published online: 9 March 2019
© Springer-Verlag GmbH Austria, part of Springer Nature 2019

Abstract

A fluorometric method is described for the determination of the tumor biomarker mucin 1 (MUC1). It is based on signal amplification of the hybridization chain reaction (HCR), and the interaction between a luminescent ruthenium(II) complex and CdZnTeS quantum dots (QDs). If MUC1 bind to the biotin-labeled aptamer, it will initiate HCR with hairpins H₁ and H₂ to form a long-range dsDNA. The long nucleic acid chains are then linked on the surface of streptavidin-modified magnetic microparticles (MMPs) through streptavidin-biotin interaction. The luminescent ruthenium(II) complex is then embedded in the long dsDNA linked to the MMPs. Hence, there is little Ru complex in the supernatant after magnetic separation, and the fluorescence of the CdZnTeS QDs (best measured at excitation/emission wavelengths of 350/530 nm) is only slightly quenched. In the absence of target, the fluorescence of the CdZnTeS QDs is strongly quenched. Fluorescence increases linearly in the 0.2–100 ng·mL⁻¹ MUC1 concentration range, and the LOD is 0.13 ng·mL⁻¹ (at S/N = 3). The method was applied to the determination of MUC1 in spiked human serum samples.

Keywords Mucin 1 aptamer · Quenching · HCR amplification · Magnetic microparticles

Introduction

Mucin 1 (MUC1) serves as an indicator in the early diagnosis of cancer [1–4]. However, it is still a challenge to detect MUC1 at the early stage, as the concentration of MUC1 is usually very low. Therefore, it is critical to develop a novel method to detect MUC1 sensitively and simply. Various methods for MUC1 detection have been developed, such as enzyme-linked immunosorbent assay (ELISA) [5], surface

enhanced Raman scattering (SERS) [6], single molecular force spectroscopy (SMFS) [7], fluorescence (FL) [8, 9] and electrochemical techniques [10, 11]. Among the above methods, the fluorescent technique has attracted great attention due to the advantages of simpleness, efficiency and convenience.

Aptamers are oligonucleotides or peptide molecules and have special affinity with different targets. What's more, aptamers have excellent advantages compared with antibodies, such as low cost, easy modification, small size, stability and lack of immunogenicity. Many successful aptasensors were reported for MUC1 detection [12–16]. These strategies were used for efficient and sensitive detection of MUC1 due to the specific binding of aptamers to MUC1. However, there were some details to be improved. For example, some of them need to immobilize DNA on the surface of the material, which had high spatial hindrance and low combined freedom, leading to low affinity efficiency between aptamers and proteins. In addition, most of them required labeling signal molecules that might result in high background signal. So it is very vital to establish a solution to solve these problems.

Electronic supplementary material The online version of this article (<https://doi.org/10.1007/s00604-019-3347-3>) contains supplementary material, which is available to authorized users.

✉ Zhike He
zhkhe@whu.edu.cn

¹ Key Laboratory of Analytical Chemistry for Biology and Medicine (Ministry of Education), College of Chemistry and Molecular Sciences, Wuhan University, Wuhan 430072, People's Republic of China

Quantum dots (QDs) are highlighted fluorescent probes, and they have attracted widespread attention in various research areas due to their unique advantages of wide excitation and narrow emission spectra, tunable size and high quantum yields [17–21]. Ru(bpy)₂(dppx)²⁺ (bpy = 2,2'-bipyridine, dppx = 7,8-dimethyldipyrido [3,2-a:2',3'-c]-phenanthroline) is one of typical DNA molecular “light switches”, which can tightly bind toward DNA, especially dsDNA, and it can efficiently quench QDs via the photo induced electron transfer process. In the presence of dsDNA, Ru(bpy)₂(dppx)²⁺ is bound by dsDNA and cannot quench QDs anymore [22, 23]. Magnetic microparticles (MMPs) have been extensively applied in the detection of DNA, small molecules, proteins, and cancer cells as a useful tool [16, 24–26], due to their high surface-to-volume ratio, easy surface modification and separation characteristics. Hybridization chain reaction (HCR) is an excellent signal amplification technique and can greatly amplify signal by DNA cascade hybridization without any nucleases involvement. H₁ and H₂ can self-assemble to form long-range dsDNA in the presence of an initiator [27]. In this experiment, Ru(bpy)₂(dppx)²⁺ bound by dsDNA, independent of whether the HCR occurred or not. This reduces the quenching effect on QDs and leads to the high background signal. The streptavidin-modified MMPs can reduce the background signal significantly via the good separation performance.

Based on this principle, we developed a novel aptasensor for the detection of MUC1. In the presence of MUC1, the initiated sequence of aptamer-H₀ triggered the HCR. The HCR product, long-range dsDNA, had stronger interaction with Ru complex than single strand DNA or H₁ and H₂. Combined Ru complex, QDs and MMPs, which greatly improved the detection sensitivity, selectivity and practicability.

Experimental section

Chemicals and instruments

Trishydroxymethyl aminomethane (Tris), sodium phosphate dibasic (Na₂HPO₄), sodium phosphate monobasic (NaH₂PO₄), potassium chloride (KCl), sodium chloride (NaCl), mucin 1 (MUC1), Tween-20, N-acetyl-L-cysteine (NAC), 4,5-Dimethylthyl-o-phenylene-diamine and 2,3-dimercaptopropane-2,3-dimercaptopropane-1-sulfonate (DMPS) were purchased from Sigma-Aldrich (USA.; <https://www.sigmaaldrich.com>). All above of them were analytical-reagent grade or better. CdCl₂·2.5H₂O, ZnCl₂, Na₂TeO₃ and hydrochloric acid was purchased from Sinopharm Chemical Reagent Co., Ltd. (Shanghai, China; <http://www.sinoreagent.com>). Meso-2,3-dimercaptosuccinic acid (DMSA) was purchased from Aladdin Chemistry Co., Ltd. (China; <http://www.aladdin-e.com>). The streptavidin-modified magnetic

microparticles (MMPs) (1 μm, 10 mg·mL⁻¹) were obtained from Invitrogen (Norway; <https://www.thermofisher.com>).

Different sequences of the oligonucleotides were synthesized by Sangon Biotechnology Co. Ltd. (Shanghai, China; <https://www.sangon.com>) and purified by high performance liquid chromatography (HPLC). The sequences of the oligonucleotides in this experiment were as follows:

Aptamer-H₀: 5'-TGA GGT AGT AGG TTG TAT AGT TGC AGT TGA TCC TTT GGA TAC CCT GGA ACT ATA CAA CCT ACT ACC TCA AAA AA-biotin-3',
Hairpin H₁: 5'-AGT AGG TTG TAT AGT TCA AAG TAA CTA TAC AAC CTA CTA CCT CA-3',
Hairpin H₂: 5'-ACT TTG AAC TAT ACA ACC TAC TTG AGG TAG TAG GTT GTA TAG TT-3'.

Ultrapure water (18.2 MΩ·cm) was produced by a Milli-Q Academic purification set (Millipore, USA). Fluorescence emission spectrum was measured with a RF-6000 PC spectrophotometer (Shimadzu, Japan). The Fluorescence intensity was measured by exciting the sample at 350 nm. The slits for excitation and emission were set at 10 and 5 nm, respectively. UV–vis absorption spectrum data was performed on a UV-2550 spectrophotometer (Shimadzu, Japan). Transmission electron microscopy (TEM) and high-resolution (HR) TEM images were obtained on a JEM-2100 electron microscope (Japan).

Synthesis of the Ru(II) complex and CdZnTeS QDs

Ru(bpy)₂(dppx)²⁺ complex and CdZnTeS QDs were synthesized according to our previous reported method [21, 28, 29], respectively. The experimental procedures were described in supporting information (SI).

CdZnTeS QDs were dissolved in Tris buffer 1 (Tris 20 mM, pH 7.4) for further use.

MUC1 detection

Firstly, DNA sequence H₁, H₂ and biotin-labeled aptamer-H₀ were heated at 90 °C for 10 min, respectively. Then the solution was cooled to room temperature for 1 h before use. Different concentration of MUC1 was mixed with 10 nM aptamer-H₀ in PBS 1 (NaH₂PO₄ 100 mM, Na₂HPO₄ 100 mM, KCl 100 mM, pH 8.0) for 1 h at 37 °C, respectively. After that, 1 μM H₁ and 1 μM H₂ in 200 μL Tris buffer 2 (Tris 20 mM, NaCl 200 mM, pH 7.5) were added into above solution for 2 h at 37 °C to proceed the HCR.

Secondly, a certain amount of streptavidin-modified MMPs were washed three times with 100 μL PBS 2 (NaH₂PO₄ 10 mM, Na₂HPO₄ 10 mM, NaCl 15 mM, pH 7.4), then they were mixed with the HCR products, respectively. After incubating at 37 °C with gentle shaking for 30 min, the conjugated MMPs were washed three times with

400 μL washing buffer (Tris 10 mM, NaCl 100 mM, Tween-20 0.01% (w/v), pH 7.5).

After the redundant DNA that absorbed on the surface of the MMPs were removed, 20 μL of 0.1 mM $\text{Ru}(\text{bpy})_2(\text{dppx})^{2+}$ was mixed with the MMPs in 360 μL Tris buffer 1 for 30 min with gentle shaking. Finally, 7.5 nM CdZnTeS QDs were added into the supernatant which had been separated with a magnet. The fluorescence intensity of the supernatant was implemented by RF-6000 PC spectrophotometer (measured at excitation/emission wavelengths of 340/530 nm).

Results and discussion

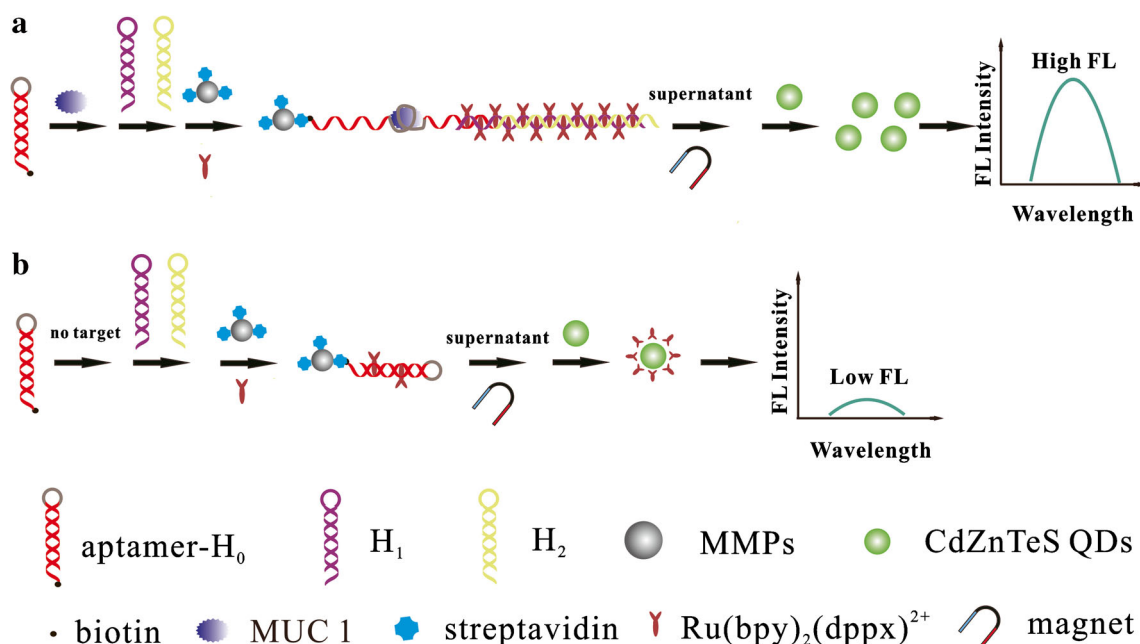
Working principle

The principle of MUC1 detection is illustrated in Scheme 1. The detection system includes biotin-labeled aptamer- H_0 , hairpins H_1 and H_2 , streptavidin-modified MMPs, $\text{Ru}(\text{bpy})_2(\text{dppx})^{2+}$ and CdZnTeS QDs. The sequence of DNA in this experiment referred the method of Ma C et al. [8]. The structure of H_0 includes stem and loop, and the sequence of aptamer is in the loop of H_0 . In the absence of MUC1, the biotin-labeled aptamer- H_0 kept stable hairpin structure from proceeding HCR with H_1 and H_2 . When streptavidin-modified MMPs were mixed with above solution, only biotin-labeled aptamer- H_0 were linked on the surface of streptavidin-modified MMPs. Subsequently, $\text{Ru}(\text{bpy})_2(\text{dppx})^{2+}$ was mixed with

the above MMPs under stirring. There were a large amount of $\text{Ru}(\text{bpy})_2(\text{dppx})^{2+}$ in the supernatant after magnetic separation due to the failure of embedding in dsDNA. After CdZnTeS QDs were mixed with the supernatant, the fluorescence intensity of CdZnTeS QDs was at a low level, as Ru complex highly quenched CdZnTeS QDs. When MUC1 is present, it binds with aptamer specifically, whose structure will be changed [30]. The initiated sequence of aptamer- H_0 will proceed HCR with H_1 and H_2 to form long-range dsDNA structures. After streptavidin-modified MMPs were mixed with the above solution, the long nucleic acid chains were linked on the surface of streptavidin-modified MMPs through streptavidin-biotin interaction. Subsequently, $\text{Ru}(\text{bpy})_2(\text{dppx})^{2+}$ was mixed with the above MMPs under stirring, then MMPs were separated with a magnet. There was little $\text{Ru}(\text{bpy})_2(\text{dppx})^{2+}$ in the supernatant, as $\text{Ru}(\text{bpy})_2(\text{dppx})^{2+}$ was embedded in dsDNA. So the fluorescence intensity of the supernatant was very high after CdZnTeS QDs were mixed with the supernatant.

Characterization of the CdZnTeS quantum dots (QDs)

The synthesized QDs were characterized by TEM, UV-vis absorption and fluorescence spectrum. As shown in Fig. 1, TEM image shows that the QDs have good monodispersion with an average size of 3.40 ± 0.40 nm. The UV-vis absorption and fluorescence spectra of CdZnTeS QDs are shown in Fig. 2, respectively. The absorption peak



Scheme 1 Schematic representation of the MUC1 detection based on fluorescent aptasensor turn-on strategy with interaction between Ru complex and QDs. The detection system includes biotin-labeled

aptamer- H_0 , hairpins H_1 and H_2 , streptavidin-modified magnetic microparticles (MMPs), $\text{Ru}(\text{bpy})_2(\text{dppx})^{2+}$ and CdZnTeS QDs

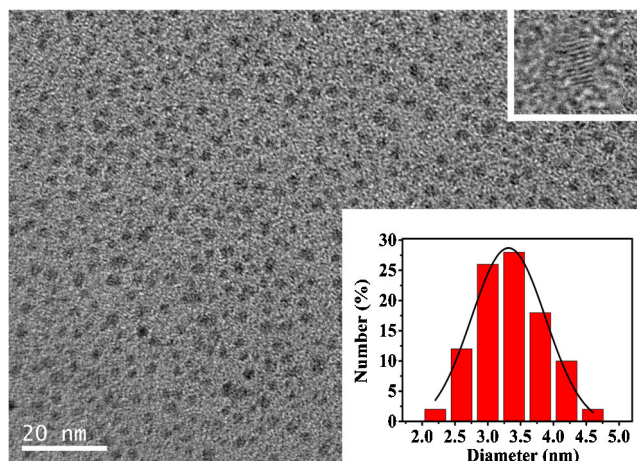


Fig. 1 TEM image of CdZnTeS QDs ($\lambda_{em} = 530$ nm), insets: HRTEM image and size distribution of QDs, respectively

is at 500 nm and the emission peak is at 530 nm. According to the absorption peak intensity, the concentration of QDs is obtained [31].

Feasibility of the design strategy

The feasibility of this strategy is shown in Fig. 3. In the absence of MUC1, only biotin-labeled aptamer- H_0 was linked on the streptavidin-modified MMPs surface, leading a lot of $\text{Ru}(\text{bpy})_2(\text{dppx})^{2+}$ dispersed in the supernatant. When CdZnTeS QDs were added into the supernatant, their fluorescence of CdZnTeS QDs was quenched by $\text{Ru}(\text{bpy})_2(\text{dppx})^{2+}$ that resulted in low fluorescence signal (Fig. 3b). When MUC1 was present without H_1 and H_2 , only small amount of Ru complex bound to the MMPs, leading to a slight peak (Fig. 3a). Only had H_1 or H_2 in the system, the fluorescence intensity of QDs was still at low level as HCR product was formed unsuccessfully (Fig. 3c and d). When MUC1 and HCR products presented

simultaneously, the supernatant with QDs showed high fluorescence signal, as a large amount of $\text{Ru}(\text{bpy})_2(\text{dppx})^{2+}$ were embedded in dsDNA (Fig. 3e). The fluorescence of QDs at different conditions is shown in the inset of Fig. 3.

Optimization of reaction conditions

The effect of $\text{Ru}(\text{bpy})_2(\text{dppx})^{2+}$ concentration on fluorescence of QDs is explored in Fig. S1. Different concentration of $\text{Ru}(\text{bpy})_2(\text{dppx})^{2+}$ (0, 1.25, 2.50, 3.75, 5, 6.25, 7.50 μM) was mixed with 7.5 nM QDs in Tris buffer 1, respectively. It reveals that the fluorescence intensity of QDs was decreased with the increasing concentration of $\text{Ru}(\text{bpy})_2(\text{dppx})^{2+}$, and the QDs showed fairly low fluorescence intensity with 5 μM $\text{Ru}(\text{bpy})_2(\text{dppx})^{2+}$. We have obtained the quenching type according to the Stern-Volmer plot (Fig. S2). The curve equation is “ $y = 0.020x^2 - 0.083x + 1.3$ ”, which is consistent with the modified Stern-Volmer equation “ $I_0/I_f = (1 + K_d[Q]) (1 + K_s[Q]) = 1 + (K_d + K_s)[Q] + K_dK_s[Q]^2$ ”. So it is indicating both static and dynamic quenching. The amount of MMPs used in the detection system was investigated. Fig. S3 shows that the fluorescence intensity of supernatant had positive correlation with the amount of MMPs from 2 to 10 μL , and the fluorescence intensity was almost stable when the adding volume of MMPs was 8 μL . The concentration of aptamer was optimized, as shown in Fig. S4. The more aptamer was, the higher efficiency of binding with MUC1 was, and the fluorescence intensity of QDs reached to a plateau when the concentration of aptamer was 10 nM. The concentrations of H_1 and H_2 were also optimized (Fig. S5). The fluorescent signal increased with the increasing concentration from 0 ~ 1 μM . However, when the concentration continued to increase, the binding efficiency between MMP and aptamer- H_0 decreased, as a large amount of DNA in the solution increased the difficulty of recognition between streptavidin-modified MMPs and

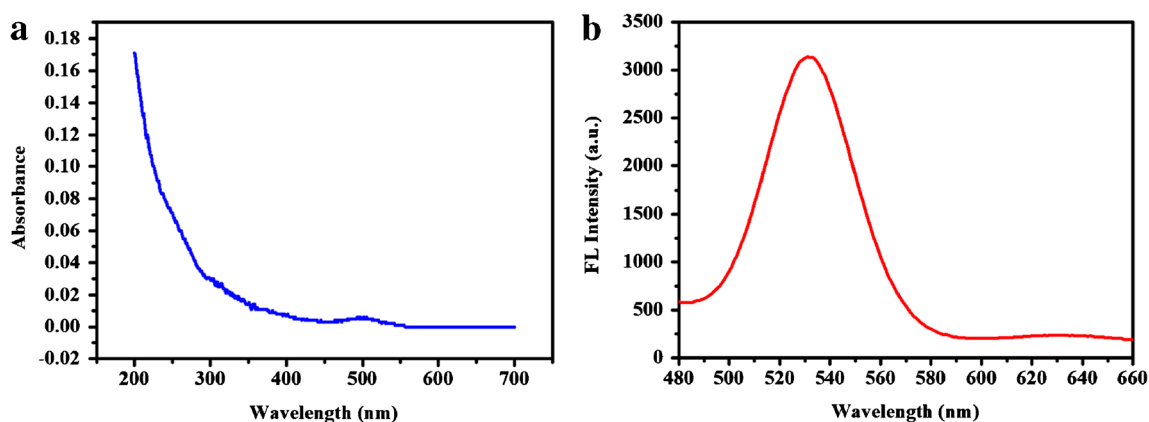


Fig. 2 UV-vis absorption (a) and fluorescence spectrum (b) of CdZnTeS QDs. The absorption peak is at 500 nm and the emission peak is at 530 nm

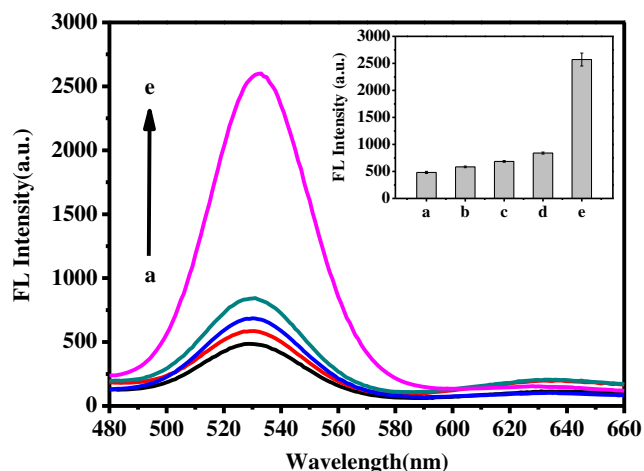


Fig. 3 Fluorescence spectra at different conditions: (a) target only; (b) H₁ + H₂; (c) target + H₂; (d) target + H₁; (e) target and H₁ + H₂; inset: fluorescence intensity of CdZnTeS QDs at different condition, respectively. The concentration of MUC1, H₁, H₂, QDs and Ru(II) complex was 100 ng·mL⁻¹, 1 μM, 1 μM, 7.5 nM and 5 μM, respectively

biotin-labeled aptamer-H₀. So the optimal concentration of H₁ and H₂ were both 1 μM.

MUC1 detection

In order to investigate the sensitivity of the detection strategy, different concentration of MUC1 mixed with aptamer-H₀ in optimal conditions was measured, respectively, as shown in Fig. 4. The fluorescence intensity of QDs was enhanced with the increasing concentration of MUC1, and the relative fluorescence intensity showed linear relationship with the concentration of MUC1 from 0.2–100 ng·mL⁻¹ (LOD = 0.13 ng·mL⁻¹, S/N = 3). Compared with the previous method (Table S1), the sensitive of this fluorescent aptasensor is better than the most of them. The result shows that this method can be used to detect MUC1 sensitively.

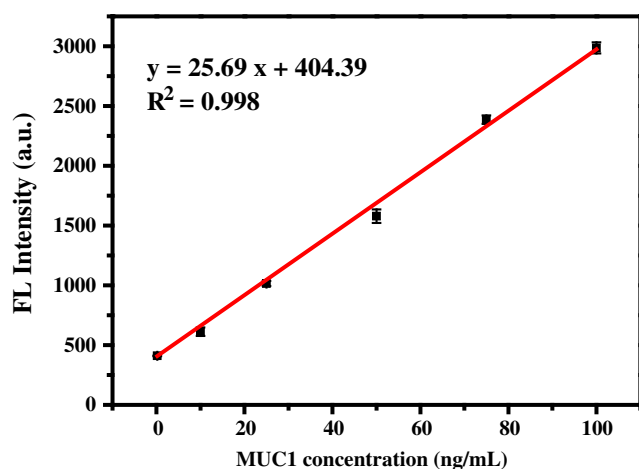


Fig. 4 The calibration plot for the determination of MUC1

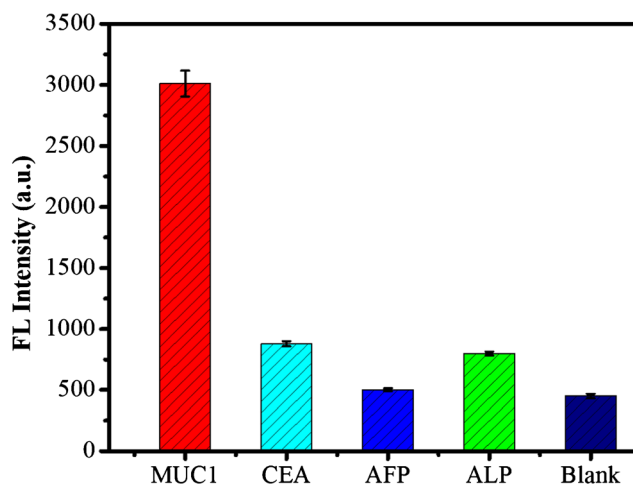


Fig. 5 The fluorescent response of this proposed method toward MUC1 and other proteins. The concentration of MUC1 was 100 ng·mL⁻¹ and other interfering substances were 1 μg·mL⁻¹

Specificity of MUC 1 detection

For proving the specificity, MUC1 and other proteins, such as AFP, CEA and ALP were tested. As shown in Fig. 5, the fluorescence intensity of QDs was effectively quenched by introducing other proteins, in spite of their concentrations were ten times as that of MUC1. So this detection method can be used for specific detection of MUC1. The reason is attributed to the unique recognition capability of the aptamer of MUC1.

MUC 1 detection in human serum

For evaluating the function of this method in complex biological environment, the fluorescent turn-on aptasensor was performed to detect MUC1 in the 20-fold-diluted human serum samples. The recovery was carried on four different levels of MUC1 samples (12.5, 25, 50 and 100 ng·mL⁻¹) with the proposed aptasensor. The recovery is in the range of 92.9–108%, and the relative standard deviation (RSD) varies from 3.00% to 6.25%, which is shown in Table 1. Therefore, the aptasensor is applicable for the determination of MUC1 in the real sample with satisfied results.

Table 1 Determination of MUC1 in 20-fold-diluted human serum samples with this fluorescence turn-on method

| Sample number | Added (ng·mL ⁻¹) | Found (ng·mL ⁻¹) | Recovery (%) | RSD (%) (n = 3) |
|---------------|------------------------------|------------------------------|--------------|-----------------|
| Serum | 12.5 | 11.6 ± 0.55 | 92.9 | 4.70 |
| | 25 | 27.1 ± 1.69 | 108 | 6.25 |
| | 50 | 48.4 ± 2.75 | 96.8 | 5.68 |
| | 100 | 107 ± 3.20 | 107 | 3.00 |

Conclusion

In summary, we establish a new method for MUC1 detection, based on signal amplification via a hybridization chain reaction and the interaction between a luminescent ruthenium(II) complex and CdZnTeS quantum dots. This MUC1 detection method doesn't require any nucleases or fluorescent labels and can be used to selectively detect MUC1 in real sample. Furthermore, this sensitive fluorescent MUC1 detection biosensor has great potential in the area of cancer diagnosis.

Acknowledgements This work was supported by the National Natural Science Foundation of China (21675119) and National Major Science and Technology Projects (2018ZX10301405).

Compliance with ethical standards The author(s) declare that they have no competing interests.

Publisher's note Springer Nature remains neutral with regard to jurisdictional claims in published maps and institutional affiliations.

References

1. Donald WK (2009) Mucins in cancer: function, prognosis and therapy. *Nat Rev Cancer* 9:874–885
2. Singh R, Bandyopadhyay D (2007) MUC1: a target molecule for cancer therapy. *Cancer Biol Ther* 6:481–486
3. Chinen AB, Guan CM, Ferrer JR, Barnaby SN, Merkel TJ, Mirkin CA (2015) Nanoparticle probes for the detection of cancer biomarkers, cells, and tissues by fluorescence. *Chem Rev* 115:10530–10574
4. Chikkaveeriah BV, Bhirde A, Morgan NY, Eden HS, Chen XY (2012) Electrochemical immunosensors for detection of cancer protein biomarkers. *ACS Nano* 6:6546–6561
5. Falahat R, Wiranowska M, Gallant ND, Toomey R, Hill R, Alcantar N (2015) A cell ELISA for the quantification of MUC1 mucin (CD227) expressed by cancer cells of epithelial and neuroectodermal origin. *Cell Immunol* 298:96–103
6. Feng JJ, Wu XL, Ma W, Kuang H, Xu LG, Xu CL (2015) A SERS active bimetallic core-satellite nanostructure for the ultrasensitive detection of Mucin-1. *Chem Commun* 51:14761–14763
7. Wang N, Zhang MM, Chen XJ, Ma XX, Li C, Zhang Z, Tang JL (2017) Mapping the interaction sites of mucin 1 and DNA aptamer by atomic force microscopy. *Analyst* 142:3800–3804
8. Ma C, Liu HY, Tian T, Song XR, Yu JH, Yan M (2016) A simple and rapid detection assay for peptides based on the specific recognition of aptamer and signal amplification of hybridization chain reaction. *Biosens Bioelectron* 83:15–18
9. He Y, Lin Y, Hong HW, Pang DW (2012) A graphene oxide-based fluorescent aptasensor for the turn-on detection of epithelial tumor marker mucin 1. *Nanoscale* 4:2054–2059
10. Hu R, Wen W, Wang QL, Xiong HY, Zhang XH, Gu HS, Wang SF (2014) Novel electrochemical aptamer biosensor based on an enzyme-gold nanoparticle dual label for the ultrasensitive detection of epithelial tumour marker MUC1. *Biosens Bioelectron* 53:384–389
11. Liu CY, Liu X, Qin Y, Deng CY, Xiang J (2016) A simple regenerable electrochemical aptasensor for the parallel and continuous detection of biomarkers. *RSC Adv* 6:58569–58476
12. Deng CY, Pi XM, Qian P, Chen XQ, Wu WM, Xiang J (2017) High-performance ratiometric electrochemical method based on the combination of signal probe and inner reference probe in one hairpin-structured DNA. *Anal Chem* 89:966–973
13. Jiang XY, Wang HJ, Wang HJ, Zhuo Y, Yuan R, Chai YQ (2017) Electrochemiluminescence biosensor based on 3-D DNA nanomachine signal probe powered by protein-aptamer binding complex for ultrasensitive mucin 1 detection. *Anal Chem* 89:4280–4286
14. Guo QJ, Li XZ, Shen CC, Zhang SB, Qi HZ, Li T, Yang MH (2015) Electrochemical immunoassay for the protein biomarker mucin 1 and for MCF-7 cancer cells based on signal enhancement by silver nanoclusters. *Microchim Acta* 182:1483–1489
15. Yazdanparast S, Benvidi A, Banaei M, Nikukar H, Tezerjani MD, Azimzadeh M (2018) Dual-aptamer based electrochemical sandwich biosensor for MCF-7 human breast cancer cells using silver nanoparticle labels and a poly(glutamic acid)/MWNT nanocomposite. *Microchim Acta* 185:405
16. Ma N, Jiang WT, Li T, Zhang ZQ, Qi HZ, Yang MH (2015) Fluorescence aggregation assay for the protein biomarker mucin 1 using carbon dot-labeled antibodies and aptamers. *Microchim Acta* 182:443–447
17. Jr MB, Moronne M, Gin P, Weiss S, Alivisatos AP (1998) Semiconductor nanocrystals as fluorescent biological labels. *Science* 281:2013–2016
18. Peng ZA, Peng XG (2001) Formation of high-quality CdTe, CdSe, and CdS nanocrystals using CdO as precursor. *J Am Chem Soc* 123:183–184
19. Liu ZY, Tang A, Wang M, Yang CH, Teng F (2015) Heating-up synthesis of cadmium-free and color-tunable quaternary and five-component Cu-In-Zn-S-based semiconductor nanocrystals. *J Mater Chem C* 3:10114–10120
20. Mao GB, Cai Q, Wang FB, Luo CL, Ji XH, He ZK (2017) One-step synthesis of Rox-DNA functionalized CdZnTeS quantum dots for the visual detection of hydrogen peroxide and blood Glucose. *Anal Chem* 89:11628–11635
21. Mao GB, Liu C, Du MY, Zhang YW, Ji XH, He ZK (2018) One-pot synthesis of the stable CdZnTeS quantum dots for the rapid and sensitive detection of copper-activated enzyme. *Talanta* 185:123–131
22. Zhao D, Chan WH, He ZK, Qiu T (2009) Quantum dot-ruthenium complex dyads: recognition of double-strand DNA through dual-color fluorescence detection. *Anal Chem* 81:3537–3543
23. Xiang X, Chen L, Zhuang QG, Ji XH, He ZK (2012) Real-time luminescence-based colorimetric determination of double-strand DNA in droplet on demand. *Biosens Bioelectron* 32:43–49
24. Liu YF, Luo M, Yan J, Xiang X, Ji XH, Zhou GH, He ZK (2013) An ultrasensitive biosensor for DNA detection based on hybridization chain reaction coupled with the efficient quenching of a ruthenium complex to CdTe quantum dots. *Chem Commun* 49:7424–7426
25. Zhang Z, Xiang X, Huang FH, Zheng MM, Xia XY, Han L (2018) Mercury ion-mediated “molecular beacon” integrating with hybridization chain reaction: application to fluorescence turn-on detection of glutathione by using quantum dots and Ru complex. *Sensors Actuators B Chem* 273:159–166
26. Liu SW, Xu NH, Tan CY, Fang W, Tan Y (2018) A sensitive colorimetric aptasensor based on trivalent peroxidase-mimic DNAzyme and magnetic nanoparticles. *Anal Chim Acta* 1018:86–93

27. Huang J, Wu YR, Chen Y, Zhu Z, Yang XH, Yang CYJ (2011) Pyrene-excimer probes based on the hybridization chain reaction for the detection of nucleic acids in complex biological fluids. *Angew Chem Int Ed* 50:401–404
28. Ling LS, He ZK, Song GW, Yuan D, Zeng YE (2000) A novel method for determination of DNA by use of molecular 'light switch' complex of $\text{Ru}(\text{bipy})_2(\text{dppx})^{2+}$. *Anal Chim Acta* 403: 209–217
29. Zhao D, Fang Y, Wang HY, He ZK (2011) Synthesis and characterization of high-quality water-soluble CdTe: Zn^{2+} quantum dots capped by N-acetyl-L-cysteine via hydrothermal method. *J Mater Chem* 21:13365–13370
30. Ferreira CSM, Matthews CS, Missailidis S (2006) DNA aptamers that bind to MUC1 tumor marker: design and characterization of MUC1-binding single-stranded DNA aptamers. *Tumour Biol* 27: 289–301
31. Yu WW, Qu LH, Guo WZ, Peng XG (2003) Experimental determination of the extinction coefficient of CdTe, CdSe, and CdS nanocrystals. *Chem Mater* 15:2854–2860